Abstract 2048

In Vitro and In Vivo Characterization of Non-Oncolytic Engineered Arenavirus Vectors for Cancer Immunotherapy

Josipa Raguz, Theresa Kleissner, Sandra Rosskopf, Mohamed Habbeddine, Katharina Lechner, Valentin Just, Donna Edwards, Igor Matushansky, J. Christoph Lampert, Klaus K. Orlinger, Henning Lauterbach

HOOKIPA Pharma Inc, New York, NY

INTRODUCTION

- Data from various preclinical models suggest that treatment with arenavirus vectors expressing tumor antigens results in sustained CD8+ T cell responses and durable antitumor responses indicative of immunologic memory that can help prevent tumor recurrence[1-4]
- HOOKIPA developed HB-200, which comprises 2 attenuated, replicating arenavirus vectors based on LCMV (HB-201) and PICV (HB-202) expressing the same non-oncogenic HPV16 E7E6 fusion protein, which have been shown in preclinical and clinical studies to elicit strong tumor antigen-specific CD8+ T cell responses[3,4]
- To further characterize the immunogenic properties of both vectors, we designed a comprehensive set of preclinical and translational experiments utilizing human PBMCs, artificial APCs, HPV16 E6- and E7-specific reporter T cells, and the TC-1 HPV mouse model
- Here, we present confirmatory nonclinical results demonstrating efficient infection and activation of human APCs and the strong immunogenicity of the engineered arenavirus platform leading to efficient tumor control in a relevant mouse model for HPV16+ cancers, which further supports the clinical development of Hookipa's novel arenavirus platform

RESULTS

Figure 1. artLCMV and artPICV Efficiently Infect and Activate Human Monocytes and Dendritic Cells Leading to MHC Class I Presentation of Vector-Encoded Antigens

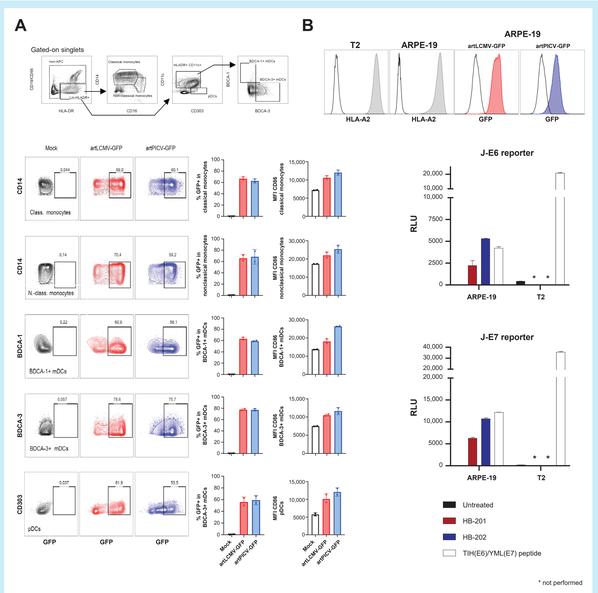

(A) PBMCs from healthy donors were infected with artLCMV-GFP or artPICV-GFP vectors using MOI5. After 20 h, different APC subsets (classical monocytes, nonclassical monocytes, BDCA-1+ mDCs, BDCA-3+ mDCs, and pDCs) were analyzed for presence of the GFP+ cells and the activation marker CD86 by flow cytometry. Mock-treated cells were used as negative control. **(B)** HLA-A2 expression of human cell lines (T2, ARPE-19) upon staining with HLA-A2 antibody (gray) or isotype control (open histogram). GFP expression levels of ARPE-19 cells 24 h after infection with artLCMV-GFP and artPICV-GFP using MOI1 **(top)**. Vector-infected ARPE-19 cells (MOI2) were cocultured for 6 h with Jurkat IL-2/NanoLuc reporter cells transgenic for HLA-A2-restricted TCRs against HPV E6 (TIHDIILECV)- and HPV E7 (YMLDLQPET)-derived epitopes **(bottom)**. Peptide-loaded T2 cells were used as positive control. RLU values are shown as mean ± SD of duplicate wells.

Figure 2. HB-201 and HB-202 Immunization Induces Strong Innate Immune Responses and Antigen-Specific T Cell Responses in Mice

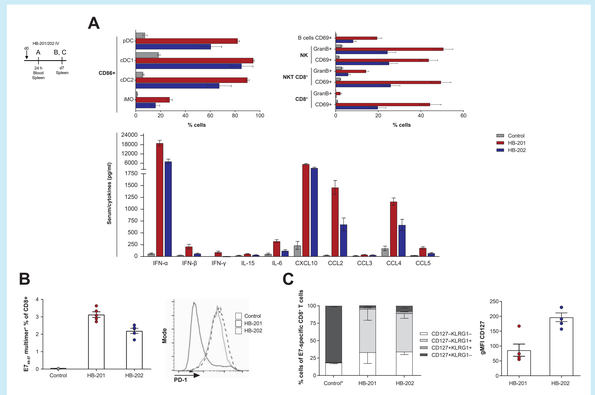

C57BL/6 mice were immunized once with 1×10^5 RCV FFU of either HB-201 or HB-202 vectors, and blood and spleen were collected 24 h and/or 7 days post immunization. **(A)** Flow cytometric characterization of activated (CD86+) myeloid cell populations **(left)** or activated (CD69+ and granzyme B+) lymphocyte cell populations **(right)** in the spleen. Serum cytokines and chemokines were measured by MSD multiplex assay **(bottom)**. **(B)** Frequency **(left)** and PD-1 expression **(right)** of $E7_{49\text{-}57}$ specific CD8+ T cells in the spleen 7 days post immunization. **(C)** Differential expression of CD127 and KLRG1 on $E7_{49\text{-}57}$ specific CD8+ T cells in immunized mice **(left)** and gMFI of CD127 **(right)**. For control samples, the total CD8+ T cell population was used. Data are shown as mean ± SEM; n=7 per group in **A** and n=5 per group in **B-C**.

Figure 3. Single Treatment With HB-201 or HB-202 Induces Remission of Established TC-1 Tumors and Mediates a Strong Abscopal Effect

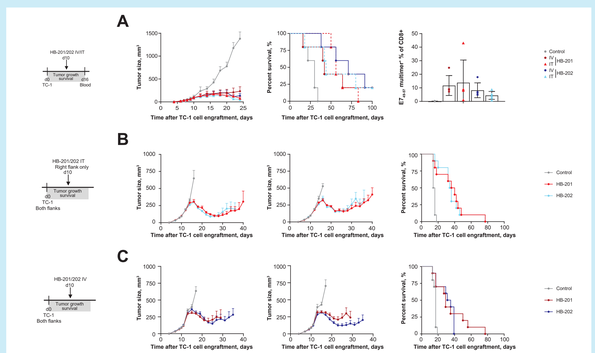

C57BL/6 mice were subcutaneously grafted with 1×10^5 TC-1 cells (HPV syngeneic mouse tumor model) in the right flank **(A)** or both flanks **(B-C)**. Animals were immunized IT or IV **(A)**, IT **(B)**, or IV **(C)** with 1×10^5 RCV FFU of either HB-201 or HB-202 vectors when tumors reached approximately 100 mm^3 (day 10). **(A)** Tumor growth **(left)** and survival **(middle)** were monitored. Frequency of $E7_{49\text{-}57}$ specific CD8+ T cells **(right)** was analyzed 6 days post immunization (day 16). To demonstrate an abscopal effect, TC-1 cells were grafted subcutaneously in both flanks **(B-C)**. Animals were treated once IT in the right flank only **(B)** or IV **(C)** with 1×10^5 RCV FFU of either HB-201 or HB-202. Tumor growth and survival were monitored. Data are shown as mean ± SEM; n=5 per group in **A** and n=10 per group in **B-C**.

Figure 4. Rapid and Strong T Cell Infiltration of Tumors After a Single Dose of HB-201 or HB-202

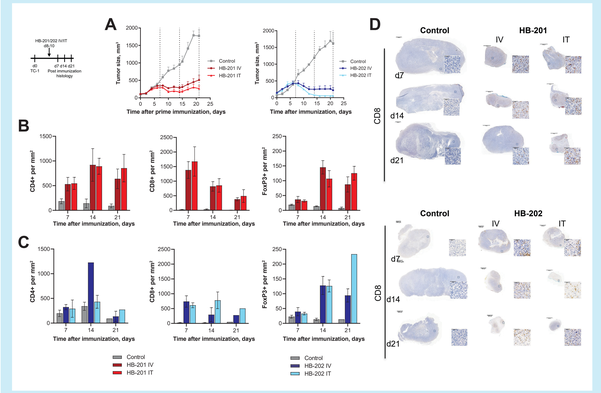

C57BL/6 mice were subcutaneously grafted with 1×10^5 TC-1 cells in the right flank. Animals were treated once IV or IT with 1×10^5 RCV FFU of either HB-201 or HB-202 when tumors reached around 100 mm^3 (days 8-10). **(A)** Tumor growth was monitored. Tumors were isolated on days 7, 14, and 21 post immunization, and tumor tissue was subjected to immunohistochemical analysis. **(B-C)** Quantification of infiltrating T cells (CD4+, CD8+, and FoxP3+). Whole slide digitization and digital analysis were performed using PANNORAMIC 250 Flash III scanner (3DHISTECH) with a 20x objective. **(D)** Representative whole CD8 staining scan. Data shown are mean ± SEM, n=2-5 per group.

Figure 5. HB-201 and HB-202 Treatment Results in T Cell Infiltration and Reprogramming of the TME

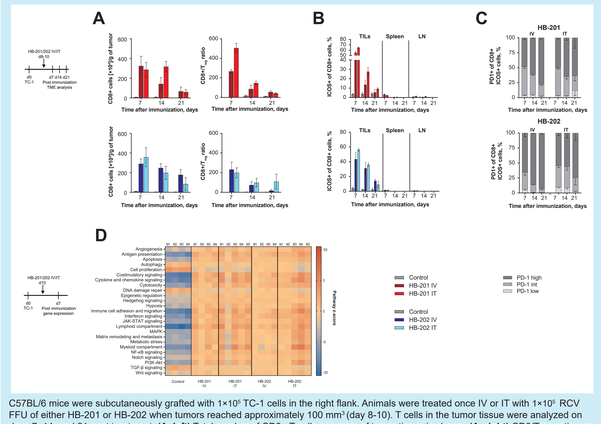

C57BL/6 mice were subcutaneously grafted with 1×10^5 TC-1 cells in the right flank. Animals were treated once IV or IT with 1×10^5 RCV FFU of either HB-201 or HB-202 when tumors reached approximately 100 mm^3 (day 8-10). T cells in the tumor tissue were analyzed on days 7, 14, and 21 post treatment. **(A, left)** Total number of CD8+ T cells per gram of tumor tissue is shown. **(A, right)** CD8/Treg ratio was calculated by dividing total number of CD8+ by total number of CD4+CD25+FoxP3+ cells. **(B)** Percentage of ICOS+ cells from total CD8+ population in TILs, spleen, and lymph nodes. **(C)** Percentage of PD-1+ subsets (low, intermediate, and high expression) from ICOS+CD8+ T cells. **(D)** Heatmap of pathway scores across all samples. Gene expression signature was evaluated using the nCounter PanCancer IO 360 Panel (Nanostring Technologies, Inc) in tumor tissue dissected 7 days after immunization. Each lane represents 1 sample, and samples are grouped according to treatment as indicated at the bottom of the heatmap. Scores are displayed on the same scale via z-transformation. Blue indicates low scores; red indicates high scores. Data shown are mean ± SEM, n=3-5 for each time point/group.

Figure 6. Antitumor Effect of HB-201 and HB-202 Treatment Is Mediated Through CD8+ T Cells

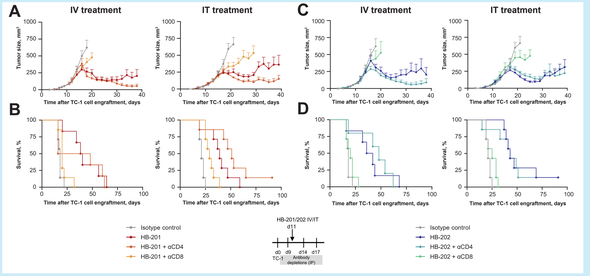

C57BL/6 mice were subcutaneously grafted with 1×10^5 TC-1 cells in the right flank. On day 11 animals were treated once IV or IT with 1×10^5 RCV FFU of either HB-201 or HB-202. Mice were depleted of T cell lineages through administration of anti-CD8- or anti-CD4-depleting antibodies. Isotype antibodies were used as control. Antibodies were administered IP on days 9, 14, and 17 of the study. Tumor growth **(A, C)** and survival **(B, D)** were monitored. **(B)** Data shown are mean ± SEM, n=7 per group.

Figure 7. HB-201 and HB-202 Treatment Synergizes With Cisplatin Chemotherapy

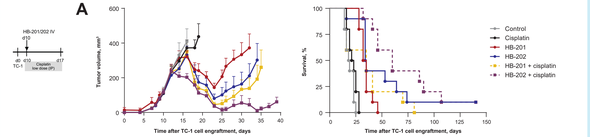

C57BL/6 mice were subcutaneously grafted with 1×10^5 TC-1 cells in the right flank. On day 10 animals were treated once IV with 1×10^5 RCV FFU of either HB-201 or HB-202 when tumors reached approximately 100 mm^3. Low-dose cisplatin (80 µg) was administered IP twice, on the day of immunization and 7 days later. Tumor growth **(A)** and survival **(B)** were monitored. **(B)** Data shown are mean ± SEM, n=10 per group.

CONCLUSIONS

- Replicating LCMV- and PICV-based vectors efficiently infect and activate human monocytes and DCs, leading to MHC class I presentation of encoded antigens
- HPV16 E7E6 encoding, replicating arenavirus-based vectors, HB-201 and HB-202, are highly immunogenic and show excellent therapeutic efficacy after a single injection independent of the route of administration in a preclinical model of HPV16-associated cancer
- Systemic administration of both vectors efficiently activate innate and adaptive immune cells, leading to rapid and strong production of type I interferons and CXCL10, an important cytokine for leukocyte trafficking and tissue homing. Responses to HB-202 were slightly lower compared with HB-201
- Independently of the route of administration (IV or IT), both vectors induce massive infiltration of CD8+ T cells into the tumor tissue and lead to reprogramming of the TME
- HB-201 and HB-202 treatments synergize with cisplatin chemotherapy
- These HPV16 targeted vectors represent a powerful new modality in tumor immunotherapy and are currently being evaluated in a Phase 1/2 study in patients with treatment-refractory HPV16+ cancers (NCT04180215; see poster #3284)[5]

Presented at the AACR Annual Meeting; April 8-13, 2022; New Orleans, LA.

ABBREVIATIONS

APC, antigen-presenting cell; ARPE-19, human retinal pigment epithelial cell line; BDCA, blood dendritic cell antigen; FFU, focus-forming unit; GFP, green fluorescent protein; gMFI, geometric mean fluorescence intensity; HLA, human leukocyte antigen; HPV, human papillomavirus; ICOS, inducible T cell costimulator; IP, intraperitoneal; IT, intratumoral; IV, intravenous; KLRG1, human killer cell lectin-like receptor G1; LCMV, lymphocytic choriomeningitis virus; LN, lymph node; mDC, myeloid dendritic cell; NK, natural killer; pDC, plasmacytoid dendritic cell; PBMC, peripheral blood mononuclear cell; PD-1, programmed death ligand; PICV, Pichinde virus; RCV, replication competent virus; RLU, relative light unit; SEM, standard error of mean; TIL, tumor-infiltrating lymphocyte; TME, tumor microenvironment.

REFERENCES

1. Bonilla WV, et al. *Cell Rep Med*. 2021;2:100209. 2. Kallert SM, et al. *Nat Commun*. 2017;8:15327.
3. Schmidt S, et al. *Oncoimmunology*. 2020;9:1809960. 4. Lauterbach H, et al. *Front Oncol*. 2021;11:732166.
5. ClinicalTrials.gov. Accessed March 1, 2022. https://clinicaltrials.gov/ct2/show/NCT04180215.

ACKNOWLEDGMENTS

We thank Katell Huang and Judith Strauss for scientific input and all members of the Preclinical R&D department at HOOKIP for excellent support of the experiments. We thank Tara Ruest, PhD, from ScientificPathways for medical editorial assistance with this presentation. This support was funded by HOOKIPA Pharma in accordance with Good Publication Practice (GPP3) (https://www.ismpp.org/gpp3) guidelines and International Committee of Medical Journal Editors recommendations.